



## Validating the LDi and LCi Indices in the Southern Hemisphere

E. Nahayo<sup>1</sup> , A. Guerrero<sup>2</sup> , S. Lotz<sup>1</sup> , C. Cid<sup>2</sup> , M. Tshisaphungo<sup>1</sup> , and E. Saiz<sup>2</sup> 

<sup>1</sup>South African National Space Agency (SANSA), Hermanus, South Africa, <sup>2</sup>Space Weather Research Group, Physics and Mathematics Department, Universidad de Alcalá, Alcalá de Henares, Spain

### Key Points:

- Geomagnetic indices Local Disturbance index (LDi) and Local Current index (LCi) successfully now-cast local geomagnetic disturbances and geomagnetically induced currents (GICs) respectively in the Southern Hemisphere
- Comparison to measured GIC shows that LCi seems to perform slightly better than  $dH/dt$  as a proxy for GIC
- We present a method for rederiving SYM-H indices using the LDi index

### Correspondence to:

E. Nahayo,  
enahayo@sansa.org.za

### Citation:

Nahayo, E., Guerrero, A., Lotz, S., Cid, C., Tshisaphungo, M., & Saiz, E. (2022). Validating the LDi and LCi indices in the Southern Hemisphere. *Space Weather*, 20, e2022SW003092. <https://doi.org/10.1029/2022SW003092>

Received 11 MAR 2022

Accepted 6 SEP 2022

**Abstract** The validation of the Local Disturbance index (LDi) and its first time derivative Local Current index (LCi) is performed in the Southern Hemisphere. Two South African magnetic observatories, Hermanus and Hartebeesthoek contributed data for this study, and two South African power stations, Grassridge and Matimba, provided geomagnetically induced current (GIC) data. This validation focused on two major geomagnetic storms, Halloween and Saint Patrick's Day events that occurred in October 2003 and March 2015, respectively. The comparative evaluation of the LDi and LCi indices was executed with the help of the local horizontal component ( $H$ ) and also comparing them to the global index SYM-H. A direct comparison to measured GIC shows that LCi performs slightly better than  $dH/dt$  as a proxy for GIC. The comparison of the LDi 1-hr magnetic disturbances values to ones calculated applying a Linear phase Robust Non-Smoothing method to the  $H$  component yields a Pearson correlation coefficient  $R$  greater than 0.960 for different groups of magnetic storms based on intensity. The estimated SYM-H index from LDi data showed a possible difference of about 300 nT from the published SYM-H index values around 20:00 UT on 29 October 2003, during the Halloween storm. This study has shown that the LDi and LCi indices, developed in the Northern Hemisphere, can be calculated at similar latitudes in the Southern Hemisphere for studying local space weather conditions and now-casting successfully local geomagnetic events.

**Plain Language Summary** The local indices Local Disturbance index and Local Current index, that were developed in Northern Hemisphere (Spain), have been successfully validated to be used in Southern Hemisphere at similar geomagnetic latitudes. This validation was carried out with the help of geomagnetic data from two South African geomagnetic observatories, Hermanus and Hartebeesthoek, and geomagnetically induced current data from two South African power stations, Grassridge and Matimba, recorded during two major geomagnetic storms, Halloween in October 2003 and Saint Patrick's Day in March 2015. The results show that these indices can now-cast successfully local space weather events better than the global geomagnetic activity indices like SYM-H.

## 1. Introduction

Geomagnetic indices are used by the scientific community to quantify the disturbances caused by solar activity on terrestrial surface. The initial 3-hr local  $K$  index, developed to provide an objective and quantitative monitoring of the irregular variations of the transient geomagnetic field observed in a given place was followed by a plethora of indices, including planetary indices, like  $K_p$  index (Bartels & Veldkamp, 1949), or those considered as proxies of the enhancement of specific magnetospheric currents like the Disturbance Storm Time index (Dst) (Sugiura, 1964) for the ring current, or the AE indices (Davis & Sugiura, 1966) for the auroral electrojet. Nowadays, the interest in quantifying geomagnetic disturbances is not limited to the scientific community as these disturbances are one of the space weather hazards affecting several technological systems. In this scenario Cid et al. (2020) developed two new geomagnetic indices: the Local Disturbance index (LDi), for nowcasting local geomagnetic disturbances at mid-latitudes, and the Local Current index (LCi), as a proxy for the geomagnetically induced currents (GICs) risk.

The LDi index is defined as a local geomagnetic disturbance index for any location at mid-latitude. It is computed by subtracting the solar regular variation and a baseline from the 1-min horizontal component of the geomagnetic field ( $H$ ) as shown below:

$$LDi = H - Sr - Baseline \quad (1)$$

© 2022. The Authors.

This is an open access article under the terms of the [Creative Commons Attribution-NonCommercial-NoDerivs License](https://creativecommons.org/licenses/by-nc-nd/4.0/), which permits use and distribution in any medium, provided the original work is properly cited, the use is non-commercial and no modifications or adaptations are made.

with  $S_r$  the solar regular daily curve and *Baseline* the long duration variation.

The solar quiet magnetic field variations, known also as solar regular variations, arise from daytime electric currents generated in the low-latitude to mid-latitude ionosphere, resulting from an upper atmosphere dynamo, which produces a regular current pattern that manifests itself as regular magnetic variations on the ground (Cnossen & Matzka, 2016). The removal of this regular variations is usually done by subtracting the so-called official quiet days for a month, which are unknown before that month has concluded. At mid-latitude locations (as in the case of Spain or South Africa) close to the foci (one at every hemisphere) of the Sq-current system, diurnal variation is highly varying from 1 day to another making difficult its removal in real time. The main goal of the LDi index was to be able to remove daily variation from local magnetic records in real time from a Spanish location based on the data recorded until that time as input. In this procedure, the  $S_r$  variation curve is obtained by fitting a model based on a spline with eight knots to the data. If the fitting is not good enough, it means it is not a quiet day, and then the procedure does not use the fitted result and takes the most recent quiet day curve. The *Baseline* is obtained by averaging quiet days and obtaining a spline with four knots per year. The index serves as a proxy for the disturbed local H-component, with local time dependence removed. More detailed information can be found in the complementary information of Cid et al. (2020). Once the LDi has been obtained, the LCI is defined as the centered discrete time derivative of LDi:

$$LCi(t) = \frac{LDi(t+1) - LDi(t-1)}{\Delta t}, \quad (2)$$

where  $\Delta t$  is 2 min.

The development of these two indices, LDi and LCI, was performed in a close collaboration between the Academia and the sole transmission agent and operator of the Spanish electricity system (Red Eléctrica de España, REE), that is, a final user of affected electric utilities in Spain. Indeed, the main goal for the development of these indices was not to provide a proxy for a scientific study (although this use was not discarded), but to provide a useful proxy to deal with GICs hazard for the specific company and the region of the Iberian Peninsula. Several steps were followed toward satisfying the needs of REE in close cooperation between researchers and the industry users, which can be tracked following the Application Usability Level (AUL) framework (Halford et al., 2019). The LCI index was validated using GICs data recorded at the neutral of a transformer located in Spain (43.2°N, 8.4°W). Nevertheless, the available data set, which extended from 2014 to 2015, never reached values larger than 5 A as the only large storm in that period was St Patrick's storm on 17–18 March 2015 (Cid et al., 2020).

Now an opportunity appears to validate not only the LDi and LCI index procedure with larger current values, but also in a different hemisphere due to a collaboration between the University of Alcalá (UAH) and the South African National Space Agency (SANSA). Spain and South Africa are locations with similar geomagnetic longitude and latitude but in different hemispheres. For example, using the 13th International Geomagnetic Reference Field (IGRF-13) model, the geomagnetic coordinates for magnetic observatories SPT and Hermanus (HER) are (42.2°N, 76.1°E) and (34.0°S, 85.5°E), respectively. Thus, using geomagnetic data from observatories in a different hemisphere and a larger range of GICs values allows to re-validate the procedure to obtain LDi and LCI indices and to show if the applicability of these products can be extended to other power companies at similar latitudes. In this context, the initial purpose of this paper is assessing on the suitability of the LDi and LCI indices for the Southern Hemisphere (Section 2). Then the analysis extends to a world-wide perspective by using the local responses of the magnetometers involved the SYM-H and ASY-H indices, and also those global indices, during the Halloween and St Patrick events in Section 3. Finally, Section 4 discusses our results and Section 5 presents our conclusions.

## 2. Overview of the Performance of LDi and LCI Indices in the Southern Hemisphere

The evaluation of the performance of LDi and LCI indices in the Southern Hemisphere is conducted using GICs measured at two substations in the South African grid operated by Eskom during two intense geomagnetic storms. We have also evaluated the performance by calculating 1-hr disturbances from two data sources for selected geomagnetic storms; the H-component disturbance obtained using the Linear phase Robust Non-linear Smoothing method (LRNS) (Hattingh et al., 1989) and LDi data.

Geomagnetically induced current are anomalous currents induced in grounded conductor networks which are excited when the fluctuating magnetic field (typically caused by geomagnetic activity) induces an electric field.

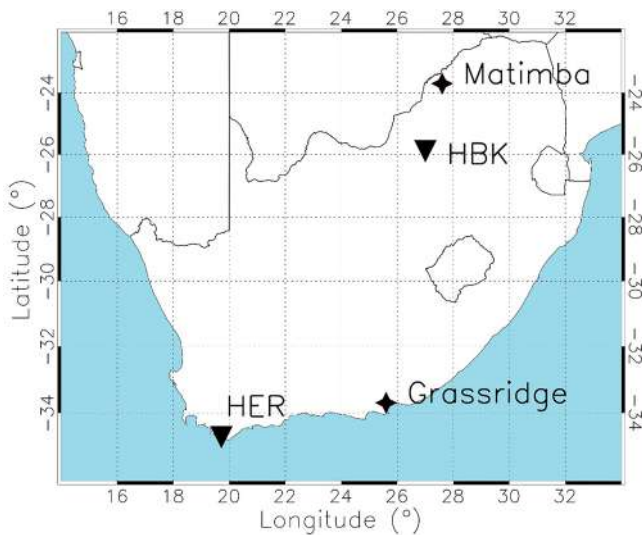


**Figure 1.** Locations of Hermanus and Hartebeesthoek magnetic observatories (black triangles) and two South African Electricity Supply Commission power stations, Matimba and Grassridge (black stars).

The spectrum of the induced field is related to the conductivity structure of the local geology (Boteler & Pirjola, 2017). In the presence of the conductor this electric field typically induces a very low frequency (quasi-DC) current in the conductor. This anomalous current can cause various problems such as increased harmonic activity and half-cycle saturation in transformers and anomalous tripping of protective relays.

In the absence of local conductivity profiles, the time derivative of the horizontal magnetic field  $H$  is routinely used as a proxy for induced electric field or GIC (Viljanen et al., 2001, 2015). The LCi index (Equation 2) is a natural proxy for GIC since it is closely related to  $dH/dt$ . In this section we compare GIC data from two substations in the South African network to LCi and  $dH/dt$  from local magnetic observatories.

### 2.1. LDi, LCi, and GICs

The performance of the LDi and LCi indices in the Southern Hemisphere was investigated by comparing geomagnetic induced currents data measured at two South African Electricity Supply Commission (ESKOM) sites, Grassridge (GRS: 33.7°S, 25.6°E) and Matimba (MAT: 23.7°S, 27.6°E) power stations (Figure 1), which have recorded good quality GIC data during geomagnetic storms. Unfortunately, there were no times both power stations recorded good quality GIC data at the same time for the study of different

responses to geomagnetic activity events. This study was performed using data recorded at two magnetic observatories, Hermanus (34.4°S, 19.2°E) and Hartebeesthoek (25.9°S, 27.7°E), during two major geomagnetic storms, the Halloween and Saint Patrick's Day storms, which occurred in October 2003 and March 2015, respectively. GICs are mostly observed in high latitude regions, but the high severity of the Halloween storm resulted in extensive damage to ESKOM power transformers located in a mid-latitude region (Falayi et al., 2017; Gaunt & Coetzee, 2007; Thomson et al., 2010).

The 2-s resolution Grassridge GIC raw data, recorded using a universal time clock (UTC), were processed to calculate 1-min data. The data were averaged and centered to the minute value by calculating the mean of 31 data points. The Matimba 1-min raw data were recorded using a local time clock, and they were processed to get the UTC timestamp.

The evaluation of the LDi index was conducted with the help of the local horizontal component ( $H$ ) measured at HER and Hartebeesthoek (HBK) magnetic observatories, and this local index was compared to the global index SYM-H (Wanliss & Showalter, 2006) to check their similarities and differences in representing the local geomagnetic activity events.

The LCi index was validated against the derivative of  $H$  and with GIC data. Five peaks in GIC data for every storm in the analysis were considered as the validation data set. With the aim of selecting the largest peaks and also separated enough for a proper validation process, the selection of five peaks from the Halloween GIC data was conducted by choosing the peaks where  $|GIC| > 7A$  and with at least 2 hr between consecutive peaks. And for the case of the Saint Patrick's day storm, the five peaks were selected where  $|GIC| > 1.5A$  and with at least 1.5 hr between consecutive peaks. Figures 2 and 3 present how the GIC peaks can be identified looking at sudden changes in the time series of indices or the  $H$  component data or their rate of change with time.

Previous studies have shown that a GIC peak occurs after within few minutes of the occurrence of the corresponding time derivative of the geomagnetic field (Kozyreva et al., 2018; Schrijver & Mitchell, 2013; Viljanen et al., 2015). The creation of electric current by the induced electric field is not easy to predict because of the non-linearity of the power transmission system and a lack of good conductivity model for an accurate estimation of the induced electric field from the time derivative of the geomagnetic field, which makes it difficult to accurately know the response of the transformers at the end of the power lines. Looking at the past work in the similar studies and considering the local case of the South African power grid system, an attempt of defining an appropriate time interval of the time derivative of the magnetic field before the corresponding GIC peak was performed. After analyzing the time delay between the occurrence times of the observed peaks in the GIC

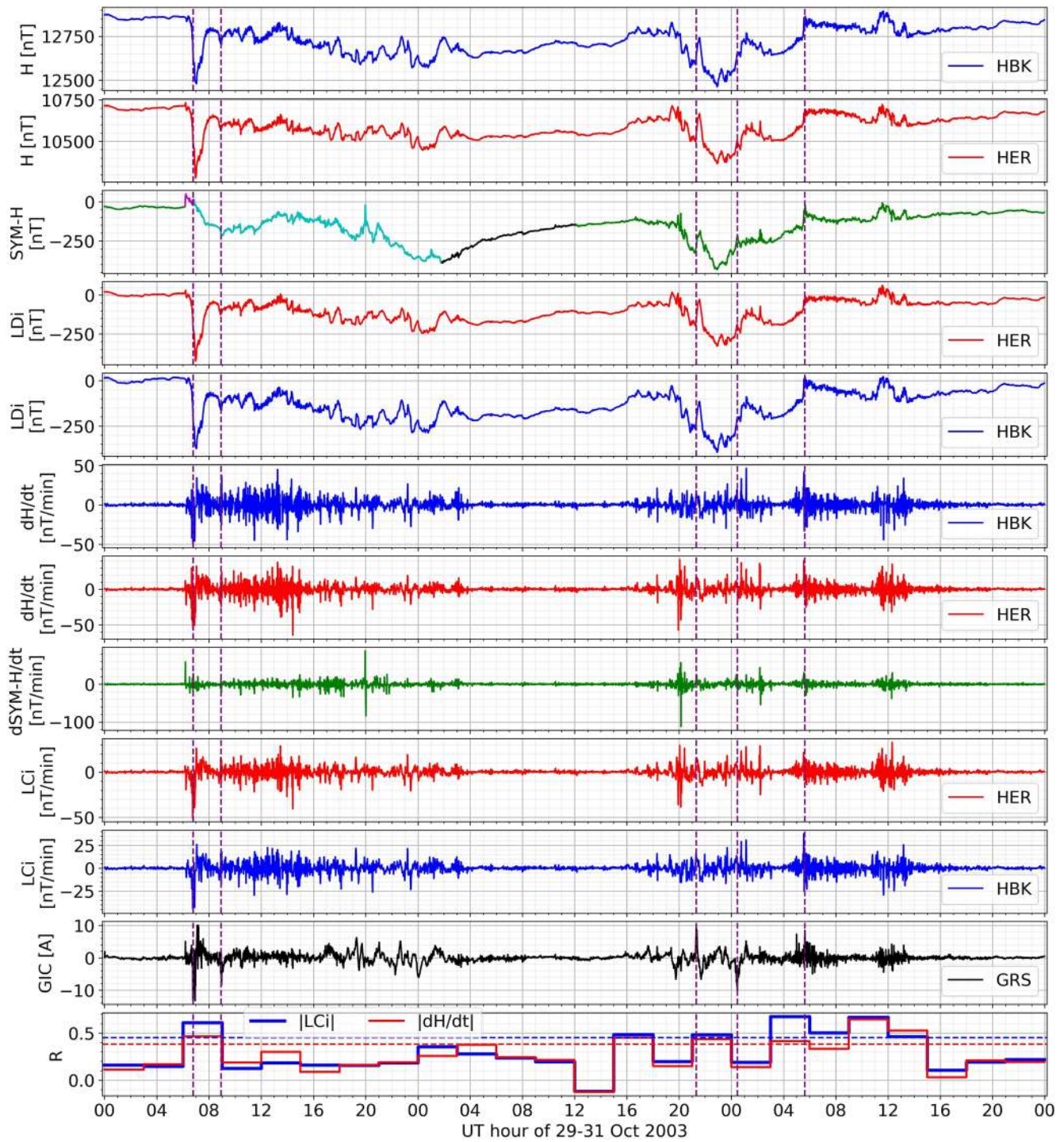


**Figure 2.** The performance of the H component and the indices Local Disturbance index (LDi) and SYM-H on the Halloween geomagnetic storm, 29–31 October 2003. From the top, there are two panels for the plots of the H component at Hermanus (HER) and Hartebeesthoek (HBK), the next three panels represent the global index SYM-H and local index LDi at HER and HBK, and five panels for their derivatives. Geomagnetically induced currents (GIC) measured at Grassridge substation is plotted in black. The last panel shows correlation between  $|LCi|$ ,  $|dH/dt|$  and  $|GIC|$  for the entire interval (dashed lines) and 180-min windows (stepped curves). Vertical dashed lines in the figure show the occurrence time of the selected five GIC peaks. Initial (magenta), main (cyan), and recovery (black) phases of the first part of the storm are indicated on the SYM-H curve (third panel from top).

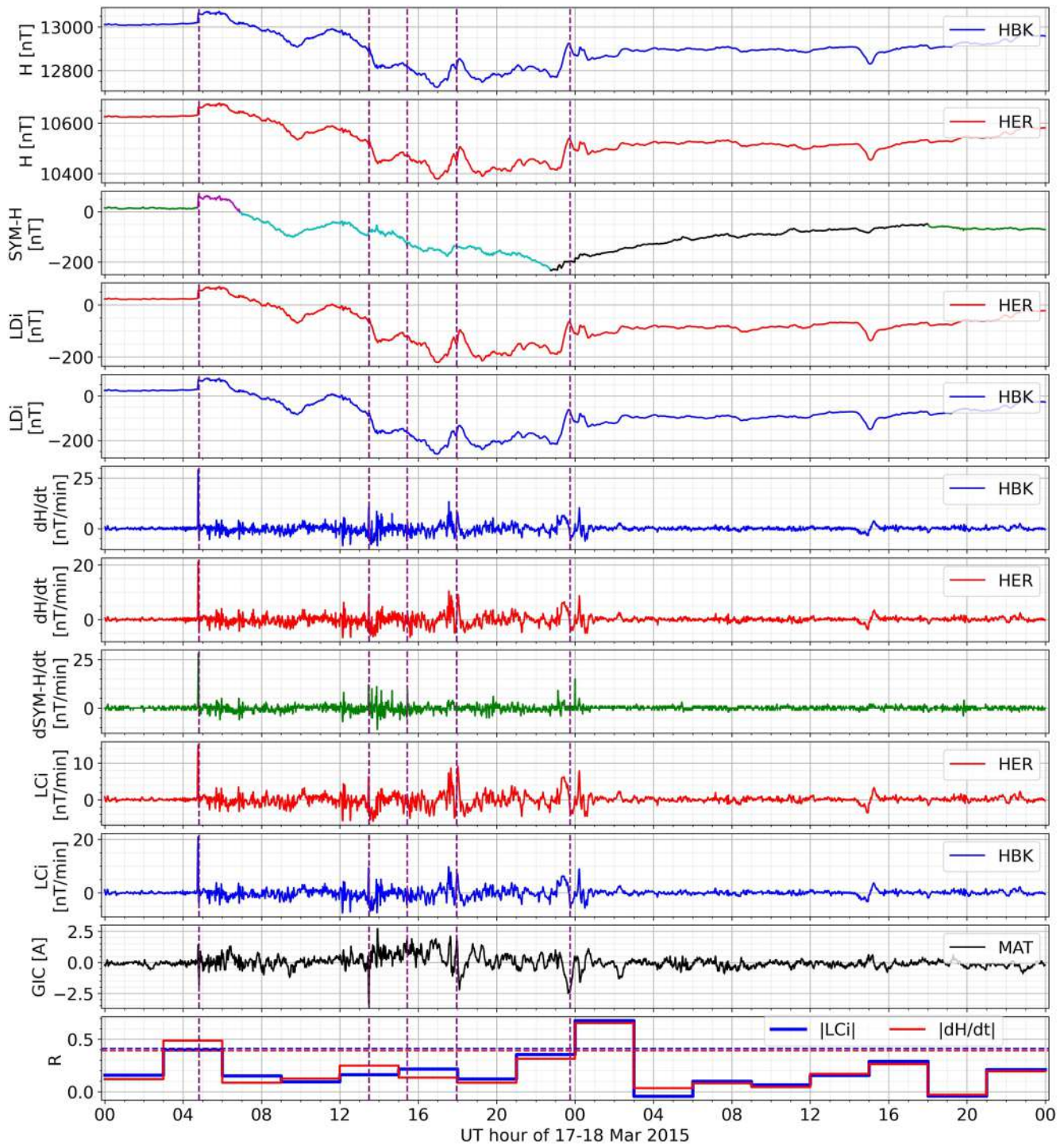


**Figure 3.** Comparison of various measurements and indices for the St. Patrick's day storm of 17–18 March 2015. Geomagnetically induced currents data (black curve) is from the Matimba substation. The layout is identical to that of Figure 2.

data and the peaks of the rate of change of the H component and indices, the maximum 1-min forward difference derivative  $ld/dt$  values within 5 min before a GIC peak is suitable to analyze the GIC response to the time derivative of the magnetic field as typical delay time between geomagnetic fluctuations and harmonic distortion is about 100 s and lower (Ciliverd et al., 2020). The central difference derivative of the H component was also calculated for the validation of the LCi index. Table 1 gives a summary of the evaluation of LDi and LCi indices

**Table 1**

*The Ten Selected Peaks in the Geomagnetically Induced Currents (GIC) Data Recorded at Grassridge and Matimba Power Stations During the Halloween and Saint Patrick's Day Geomagnetic Storms and the Maximum Absolute Rate of Change Values Calculated From  $H$ , Local Disturbance Index and SYM-H Within 5 min Before the GIC Peak Occurrence Time*

Date and time (UT)	GIC (A)	$ldH/dt$ (nT/min)		$ldLDi/dt$ (nT/min)		$ld_cH/dt$ (nT/min)		$llCi$ (nT/min)		$ldSH/dt$ (nT/min)
		HER	HBK	HER	HBK	HER	HBK	HER	HBK	
Grassridge										
29 10 2003 06:47	-12.2	54.8	49.3	54.8	49.4	50.6	44.9	50.6	45.0	28.0
29 10 2003 08:57	-7.8	24.5	37.0	24.5	37.0	15.6	18.6	15.8	18.6	21.0
30 10 2003 21:19	8.6	17.3	17.8	17.3	17.9	15.4	16.3	15.4	16.4	10.0
31 10 2003 00:28	-9.0	17.2	19.5	17.1	19.6	10.8	13.9	10.8	13.9	14.0
31 10 2003 05:38	7.5	40.6	41.7	40.6	41.6	20.8	37.8	20.8	37.7	31.0
Matimba										
17 03 2015 04:49	-1.8	21.2	29.0	21.2	28.9	14.9	20.9	14.8	20.8	28.0
17 03 2015 13:29	-3.4	9.0	10.5	9.0	10.5	6.4	9.4	6.3	9.4	12.0
17 03 2015 15:26	1.9	3.2	3.4	3.2	3.4	1.5	4.5	1.4	4.5	9.0
17 03 2015 17:58	1.9	4.3	6.8	4.4	6.8	4.1	6.3	4.1	6.2	2.0
17 03 2015 23:45	-2.3	4.2	5.9	4.2	5.9	3.4	5.1	3.4	5.1	1.0

*Note.* The notations  $ld_cH/dt$  and  $ldSH/dt$  represent the absolute values of the central difference derivative of the  $H$  component and the forward difference derivative of the SYM-H index ( $ldSYM-H/dt$ ), respectively.

during the Halloween and Saint Patrick's day geomagnetic storms and shows that the Horizontal component and all involved indices generally present a similar rate of change with time for the selected GIC peaks.

A fast glance to Table 1 allows to notice that the values of the forward derivative of  $H$  and  $LDi$  coincide (considering a range of  $\pm 1$  nT/min) for the same magnetic observatory. However, they do not coincide with the forward difference of the SYM-H or with the  $LCi$ . In the first case, the differences are due to the average process in the computation of a global index, as it is the SYM-H, which misses the local disturbances. In the second case, the differences are related to the way of computing the  $LCi$ . This index is defined as the central derivative and therefore captures the changes of the  $LDi$  index in a 2-min interval (see Equation 2). This can be noticed when comparing the absolute values of the  $LCi$  with the values of the central derivative of  $H$  in Table 1. These values coincide for any station within a range of  $\pm 2$  nT/min.

In order to validate the  $LCi$  index as a proxy for GICs, we have plotted the absolute value of the  $LCi$  at every observatory versus the absolute value of the GIC data for the 10 selected peaks (central panel in Figure 4), and also the absolute value of the forward derivative of SYM-H versus the absolute value of the GIC (bottom panel in Figure 4). While no clear correlation appears between the forward derivative of SYM-H and the GIC, the larger the absolute value of the  $LCi$ , the larger the absolute value of the GIC. However, some differences appear in the plot of  $LCi$  versus GIC that depart the trend from a linear fitting making the linear correlation coefficient  $R$  to reach a value of 0.79 in the case of HER and 0.73 for HBK. Searching for an explanation for this departure, we have compared the absolute value of  $LCi$  from HER and from HBK (top panel in Figure 4). Despite the evident high linear correlation ( $R = 0.92$ ) between  $LCi$  at both locations, it is worth to notice that some differences (up to 50%) appear between both values valorizing the local character of the index. Moreover, the slope of a linear fitting is lower than the unit (0.89), which can be associated to the labeled as "coast effect" (Gilbert, 2005) due to the proximity of HER to the ocean. These results guide us to consider that for accurate studies between GICs and geomagnetic indices, the GIC data from Matimba should be only compared to geomagnetic disturbances recorded at HBK and that the GIC data from Grassridge should be compared to HER records. Similar problems arise when trying to compare whether GICs values are better associated to  $LCi$  index or with forward derivative of  $LDi$ , that is, which time variation (1- or 2-min) of the  $H$  index provides a better proxy for GIC values.

For the rest of this work we only perform direct comparisons between the pairs HER-GRS and HBK-MAT. The distances between HER-MAT and HBK-GRS are too great to be adequately compared as regional conductivity structures may vary significantly over these vast distances.

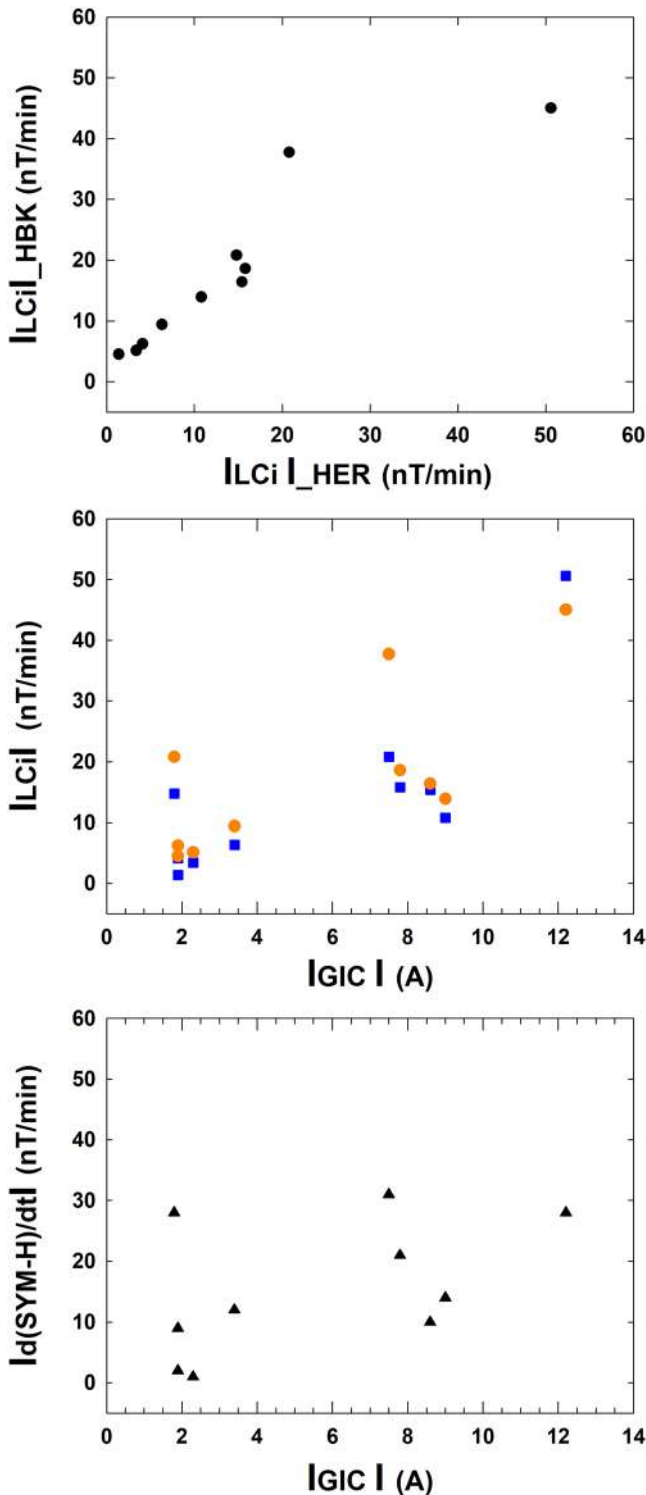


**Figure 4.** Geomagnetically induced currents-derivates. Blue square Hermanus, orange circle Hartebeesthoek.

The aim in this section is to find whether LCi is an appropriate proxy to recorded GIC and to compare that to  $dH/dt$ . For the first event (Event 1: 2003/10/29–31) we compare Grassridge GIC with the forward derivative  $dH/dt$  (forward difference) and LCi from HER (the nearest Intermagnet observatory to Grassridge). HBK  $dH/dt$  and LCi are compared to Matimba GIC for the St. Patrick's Day event (Event 2: 2015/03/17–18).

For the two events investigated the initial, main, and recovery phases were identified by visual inspection of SYM-H: The initial phase is taken as the period from storm sudden commencement (SSC) with positive SYM-H and ending when SYM-H first dips below 0 nT, indicating the start of the main phase. The end of the main phase is taken at the time of minimum SYM-H. The recovery phase is signified by a gradual return toward zero SYM-H. The phases are indicated in the color-coded sections of the SYM-H plots (third panel) of Figures 2 and 3 (see Figure 2 caption for more detail). The analysis by storm phase is done to test for systemic differences in the correlation between proxies and GIC related to storm phase. Note that for event 1 the analysis by phase is only done for the first part of the event where the initial, main and recovery phases of the first storm could be easily identified.

We calculate the Pearson correlation ( $R$ ) between the absolute values of GIC and the proxies LCi and  $dH/dt$  for the entire intervals spanning the Halloween and St Patrick's day events. This is depicted with dashed lines in the bottom panels of Figures 2 and 3. For the first event the LCi yielded significantly higher correlation with GIC than  $dH/dt$ , while the correlation is almost equal during the second event (see Table 2, column "All").

The stepped curves in Figures 2 and 3 indicate the correlation between GIC and LCi (blue) or  $dH/dt$  (red) during 180-min windowed intervals. During the March 2015 event there seems to be no clear systemic differences in the effectivity of LCi versus  $dH/dt$ , with only small deviations between the two correlation curves. During the 2003 event, however, it seems that the correlation between GIC and LCi is greater than that for (GIC,  $dH/dt$ ) especially during periods of enhanced GIC activity. We refer specifically to the periods at the start of the event (approximately 05:00–09:00 on 2003/10/29) and the storm expansion/recovery periods at 03:00–09:00 on 2003/10/31. Both these periods were characterized by high amplitude and rapid variation in induced current.

Table 2 lists the correlation between  $|GIC|$  and  $|LCi|$  or  $|dH/dt|$  by phase for the two events. The correlation for each event is listed in the third column and the correlations for separate phases are written in the last three columns. The correlation between LCi and GIC is to be greater than correlation with  $dH/dt$  for the first event—and indeed for each phase of the first storm. The initial phase particularly shows a large discrepancy between the correlations, for both events. Note however, that the initial phases are typically much shorter in duration than main and recovery phases, and therefore the data sets comprising the "Initial" intervals are small and result in less robust correlation estimates.

Differences in correlation between parameters and GIC are fairly small for all phases of the second storm—with maximum difference 0.05 for the initial phase. For this phase  $dH/dt$  yielded the higher correlation, with the (GIC, LCi) correlation slightly higher for the main and recovery phases (difference of 0.02 in both cases).

The conclusion to be gleaned from Table 2 and the bottom panels of Figures 2 and 3 is that LCi is an adequate proxy for GIC, at least as good as  $dH/dt$ , if not slightly better, in terms of linear correlation.

**Table 2**  
*Correlation Between Recorded Geomagnetically Induced Currents and Local Current Index and dH/dt for the Two Events*

Parameter	Event	All	Initial	Main	Recovery
LCi	1 (HER, GRS)	<b>0.45</b>	<b>0.76</b>	<b>0.27</b>	<b>0.38</b>
dH/dt	1 (HER, GRS)	0.38	0.42	0.20	0.36
LCi	2 (HBK, MAT)	<b>0.41</b>	0.24	<b>0.24</b>	<b>0.52</b>
dH/dt	2 (HBK, MAT)	0.39	<b>0.31</b>	0.22	0.50

*Note.* Magnetic field and GIC recordings from Hermanus and Grassridge are utilized for the first event and from Hartebeesthoek and Matimba for the second. The third column lists correlation for the entire event (“All”) and the last three columns for individual storm phases. The extent of storm phases are indicated in third panel of Figures 2 and 3 respectively. The highest correlation in each case is printed in boldface.

## 2.2. LRNS 1-hr Magnetic Disturbances

The LDi index, developed in Spain (Northern Hemisphere), is also validated in the Southern Hemisphere by comparing its 1-hr magnetic disturbances and the ones calculated from the H component. A good correlation would indicate that the LDi can represent well the local geomagnetic activity events and its method of derivation ensures a good performance in regions of similar latitudes like Southern Africa. The 1-hr magnetic disturbances are calculated by getting an amplitude range for each hour of LDi and the residual disturbed H component data after removing the solar quiet variation curve (SR) using the LRNS method (Hattingh et al., 1989).

Some case studies for different levels of severity were considered to conduct an analysis of the comparative performance evaluation of the LDi index using the LRNS method. In each group, a bar graph for 1-hr disturbance values for the H component and LDi data is plotted for a visual presentation (Figure 5), and other graphs are presented in the Appendix A. Table 2 presents the results of the Pearson linear correlation  $R$  (Freedman et al., 2007) computed

between 1-hr disturbance values from the horizontal component H and LDi data. In an attempt of checking if the value of  $R$  has any dependency on the severity of geomagnetic storms, two to three geomagnetic storms were grouped according to their levels of severity for better visualization of the results. A maximum 1-hr disturbance value (MD) was used as a proxy for the severity of a geomagnetic storm.

The analysis of results does not show any clear evidence that the agreement between 1-hr disturbance values from H and LDi depends on the severity of the geomagnetic storms. This demonstrates the consistency of the LDi performance, which is expected to produce similar 1-hr disturbance values to the ones calculated from the H component for geomagnetic storms of different levels of severity.

## 3. The World-Wide Perspective of the Event

In this section, we analyze the local and global responses of the Halloween and St Patrick events in the context of data processed by LDi and global indices processed following SYM-H and ASY-H procedures and using LDi as sources. We have obtained LDi from the current observatories involved in the definition of symmetric component (SYM) and asymmetric component (ASY) indices (except Urumqi observatory (WMQ), which is closed). Figure 6 shows the locations on the map of all the observatories. Six different sectors are identified by different colors. Some sectors include two observatories, while the purple sector only includes Honolulu Observatory (HON) and the red sector only includes Memanbetsu observatory (MMB). Observatories in the same sector share similar longitudes. This criterion is the same used for SYM and ASY indices (Iyemori, 1990).

### 3.1. Local Perspective Using LDi Indices

In Figures 7 and 8 it can be seen LDi data for all the observatories involved in the definition of SYM and ASY indices for Halloween and St Patrick events, respectively. The data have been processed with the LDi technique to remove solar regular variations and the baseline. Data from observatories in the same sector (similar longitude) are shown with the same color. For both events, we can see strong differences between locations. The differences are stronger for observatories in different sectors. For example, from 06 to 08 UT on 29 October 2003, during the Halloween event in Figure 7, we can see how BOU and TUC observatories show a positive disturbance of about 300 nT while HER and CLF show negative disturbances even greater. But the local response can also be considerably different for observatories in the same longitude. Consider for example, the disturbances between 18 UT to midnight on 30 October 2003; observatories BOU and TUC, in the same sector, show disturbances with opposite signs. The same occurs for FRD on SJG, in the same sector, during that period of time. The total difference, the sum of the absolute values, amounts to about 800 nT, which should not be overlooked. Another interesting feature is how similar can be the response in observatories in the same sector but in different hemispheres, close to their magnetic conjugate positions, like CLF and HER. This is clearly seen in both events in Figures 7 and 8, even if their responses are not similar to any other location.



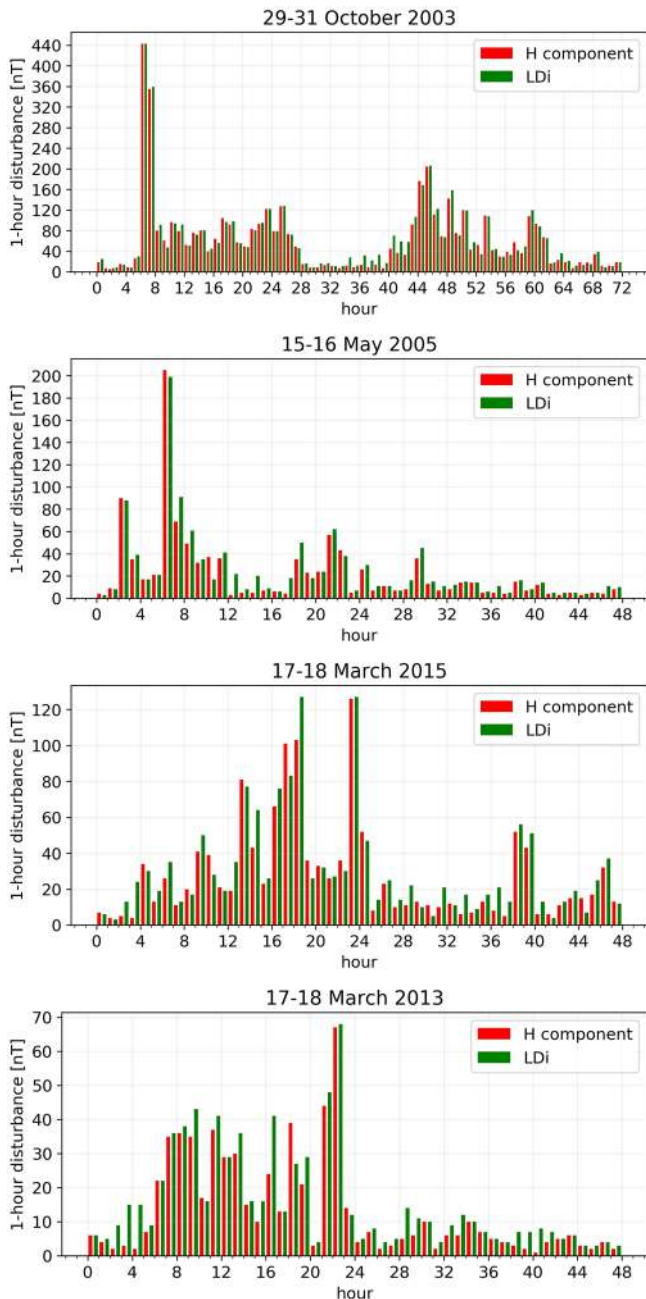


**Figure 5.** Plot of Linear phase Robust Non-linear Smoothing method and Local Disturbance index 1-hr magnetic disturbances in the H component at Hermanus magnetic observatory for four selected geomagnetic storms with different degrees of severity.

unique observatories in their sectors, but the others are subject to be included in the selection. Figure 9 shows in blue the range of values that results from all the possible SYM-H indices obtained using the LDi technique for Halloween (top) and St Patrick events (bottom). The red line is the official index from Kyoto World Data Center (<http://wdc.kugi.kyoto-u.ac.jp/>). The blue area gives also an indication of the uncertainties implied in the actual definition of the SYM-H index. The fact that observatories can be chosen without a more specific criterion makes the final index to be undetermined within the ranges shown in blue. For some periods of time, the difference can be greater than 300 nT for the Halloween event.

### 3.2. Global Perspective

In order to better evaluate the importance of the results in the previous section, we have processed the data to obtain the symmetric responses of the ring current in a similar way to SYM-H. A rough derivation procedure have been published in Iyemori (1990) and Iyemori and Rao (1996), (it is also published at Kyoto World Data Center website, although not in detail). In this last reference, dated February 2010, it is stated the following “A detailed description of the derivation and the characteristics of the indices will appear elsewhere. The following is a rough explanation of each step of the derivation.” As far as the authors are aware, no updates have been found, so we have tried to make the procedure as close as possible to the public information referenced above, dated 2010. The stations are those shown in the previous section. For the derivation of SYM-H and ASY-H, only six observatories are used, one for each longitude (color). The specific choice of observatories depends on the availability and condition of the data of the month. In the official procedure, there are four steps to create the indices:

1. Subtraction of the Earth main field and Sq field: for this step, we use directly the LDi for the observatory.
2. Coordinate transformation to a dipole system: we do not apply this transformation as it is understood to affect only the  $D$  component (declination) and not the horizontal component.
3. Calculation of the SYM: the data from the selected six observatories are averaged and corrected in latitude by the average of the cosine of the latitudes for each location. For this step, it is important to notice that in Iyemori (1990) the correction was by the cosine of the average of the latitudes instead of the average of their cosines. This can lead to big differences. As long as we know, this fact has not been reported anywhere else. It is also worth noticing that the latitude correction is applied after all the observatories have been averaged, even though it would make more sense to correct each location first and average them after the correction has been applied to each observatory data. This fact has been reported in previous works by Karinen and Mursula (2005), Mursula et al. (2008), and Häkkinen et al. (2003), for example,
4. Calculation of the ASY: the symmetric component obtained in step 3 is subtracted from the disturbance at each location (steps 1–2) and the asymmetric component is calculated as the range between the maximum and the minimum at each moment for the six stations. In this step, there are latitudinal corrections before and after subtracting the symmetric component. We do not calculate the ASY index in this work.

As stated before, the procedure involves a selection of observatories because only six take place in the derivation of the indices. The criterion for the selection is not defined unambiguously, so we have opted to create all possibilities and study the differences. Because there are four sectors with two observatories in which a choice needs to be taken, the total number of all possible combinations is 16. All combinations will have HON and MMB as they are

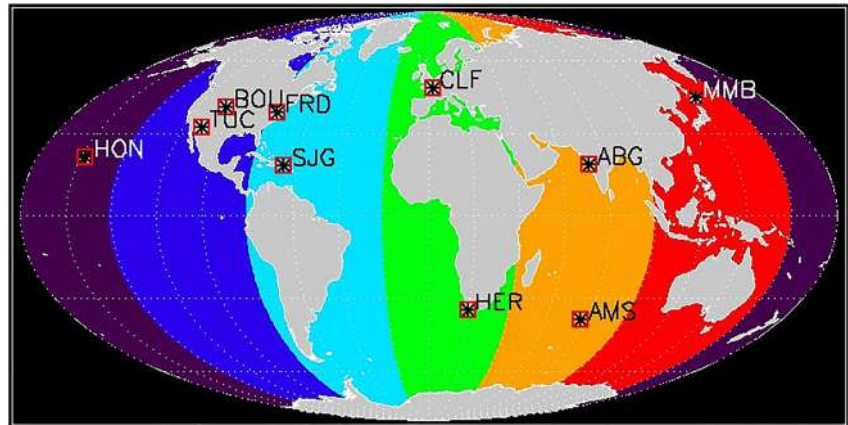


**Figure 6.** World map indicating the positions of the observatories used to derive symmetric component and asymmetric component indices. The colors indicate different longitude sectors. Only one station for each sector is used to derive the indices.

In the intervals analyzed the published SYM-H index (in red in Figure 9) is well within the ranges of possibilities of SYM-H obtained from LDi, but small intervals where the blue area is departed from the official SYM-H (e.g., during the recovery phase of 30 October 2003). Thus LDi procedure validation against SYM-H index as ground value concludes with positive results.

#### 4. Discussion

The validation of LDi and LCI indices in the Southern Hemisphere is conducted with the help of GIC data recorded at two South African power network stations, namely Grassridge and Matimba, and data from two magnetic observatories in the region, HER and HBK. The comparison of five selected major peaks in the GIC data during the Halloween and Saint Patrick's Day geomagnetic storms and the rate of change values calculated from H, LDi and the global index SYM-H reveals that for each GIC peak, there is a corresponding peak in the rate of change values.

Table 1 and Figures 2 and 3 show that the forward derivatives of the H component ( $dH/dt$ ) and LDi index ( $dLDi/dt$ ) are very similar, and it is the same for their central derivatives  $d_c H/dt$  and LCI index as these indices are calculated using local data unlike the global index SYM-H. Considering only the results for one power station, Table 1 shows that there is no clear positive correlation between the magnitude of the GIC peaks and peaks in the rate of change values calculated from indices. However, a closer look at the comparison of the presented results for Grassridge and Matimba, in Table 1, suggests a positive correlation. In the top part of Table 1, the relatively big GIC values correspond to the big values of the rate of change of indices in agreement with (Cid et al., 2020). And in the bottom part of Table 1, the relatively small values of GIC correspond to the small values of the rate of change of indices. The absence of peaks in the rate of change of indices during some time intervals corresponds to the absence of GIC peaks. This is visible in Figure 2, for time interval 4:00–16:00 UT on the 30 October 2003, and in Figure 3 and 3:00–24:00 UT on the 18 March 2015.

In a direct comparison between  $dH/dt$  and LCI as proxies to GIC we found a slight preference for LCI. Over the two geomagnetic storms studied the LCI had a slightly higher correlation with GIC than  $dH/dt$  (0.45 vs. 0.38 and 0.41 vs. 0.39). Furthermore, the results seemed to indicate that LCI has higher correlation during periods of high GIC and highly varying GIC. This is an interesting finding, but due to the small data set under consideration no specific claims are made in this regard.

On the other hand, calculated 1-hr magnetic disturbances from the H component and LDi index were compared for geomagnetic storms with different degrees of severity (Figures 5 and A1). Results in Table 3 show that the Pearson correlation coefficient  $R$  between 1-hr magnetic disturbances calculated from the H component and LDi index for all considered geomagnetic storms is greater than 0.960. Looking at  $R$  values in Table 2, there is no clear degradation of  $R$  with the degree of severity of a considered geomagnetic storm.

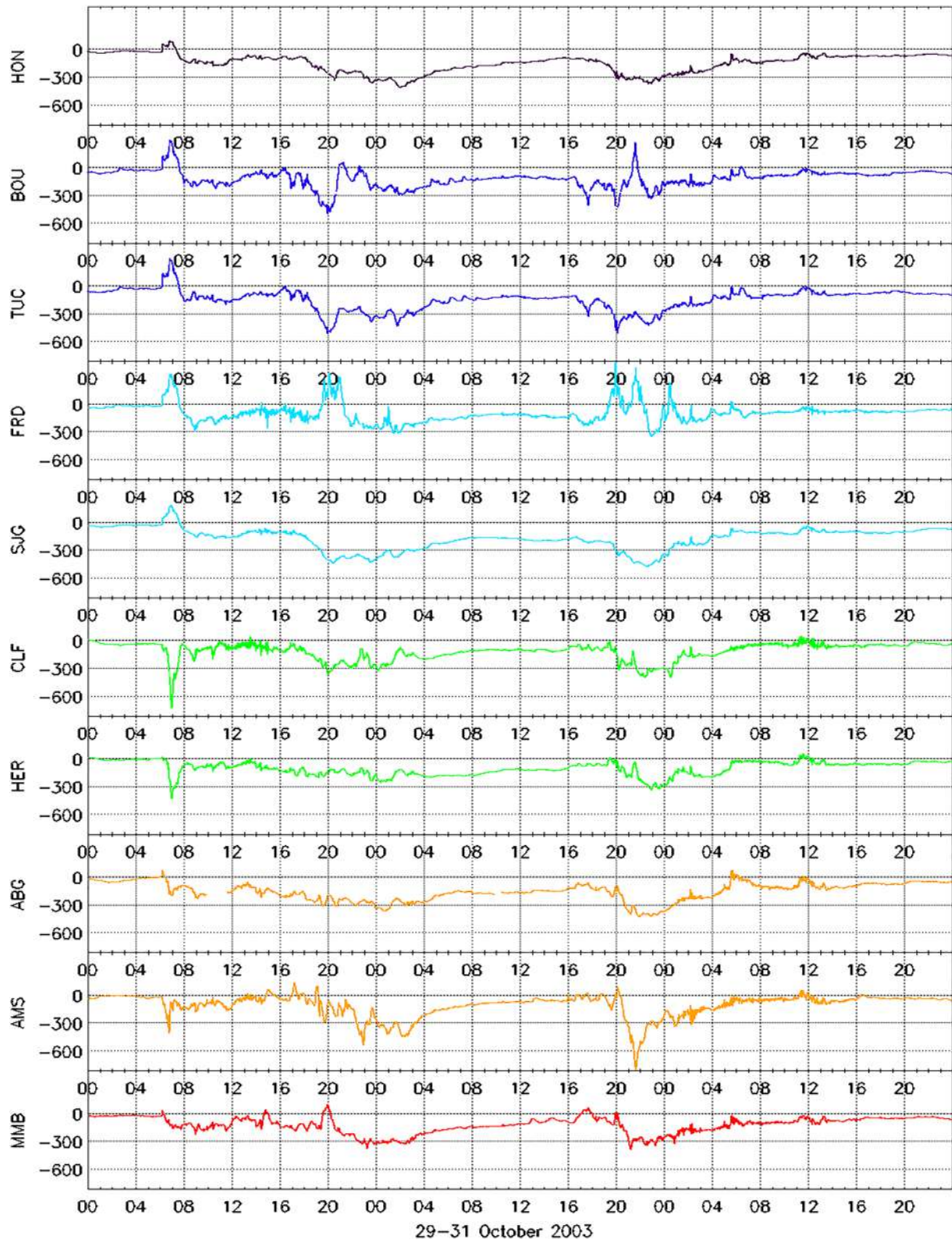


**Figure 7.** The Local Disturbance index (LDi) for the symmetric component (SYM) and asymmetric component (ASY) stations for the Halloween event (29–31 October 2003). Same color indicates similar longitude. To obtain SYM and ASY indices, a choice has to be made in order to get only one station (different color) for each of the (six) longitude sectors.

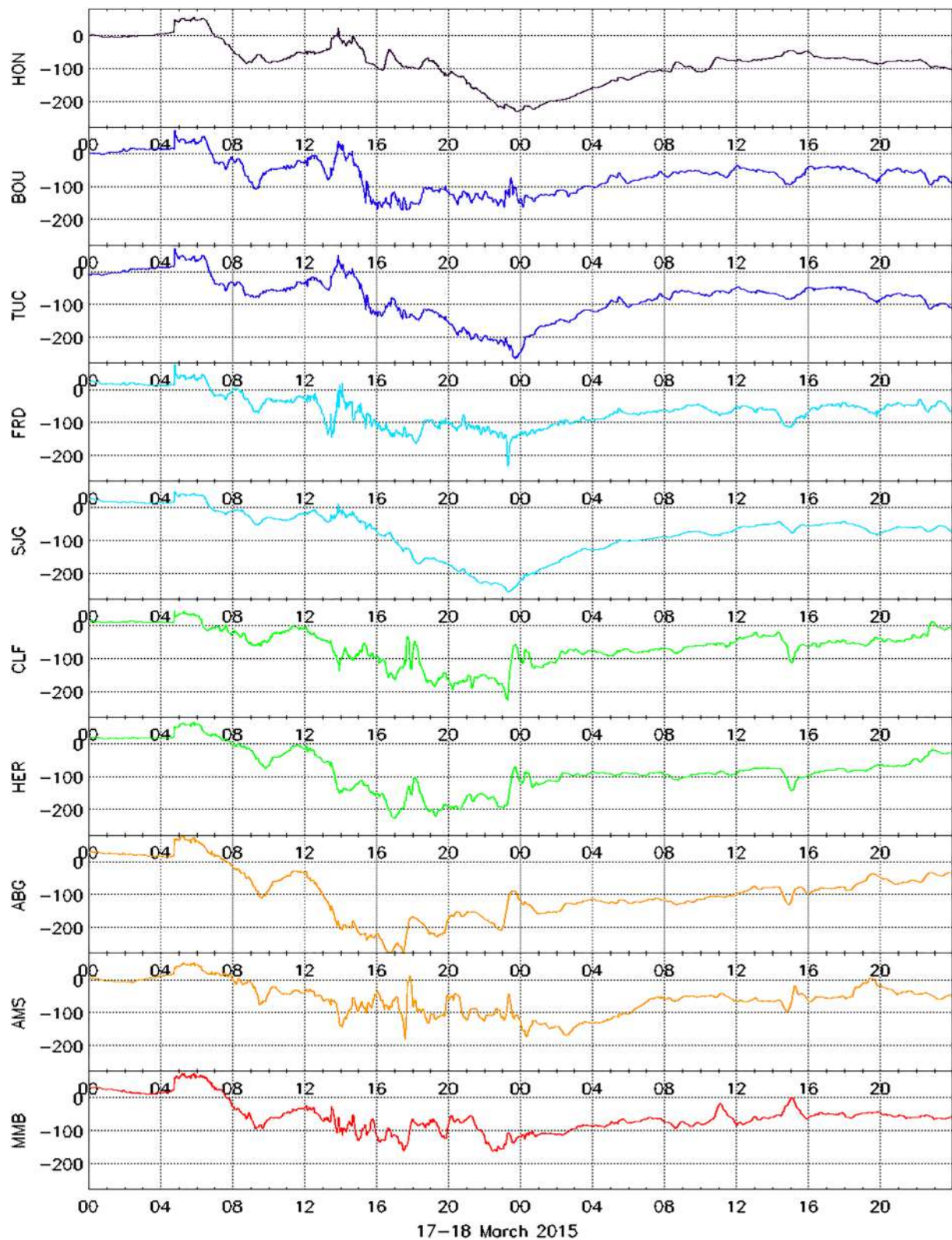


**Figure 8.** The Local Disturbance index (LDi) for the symmetric component (SYM) and asymmetric component (ASY) stations for the St. Patrick event (17–18 March 2015). Same color indicates similar longitude. To obtain SYM and ASY indices, a choice has to be made in order to get only one station (different color) for each of the (six) longitude sectors.

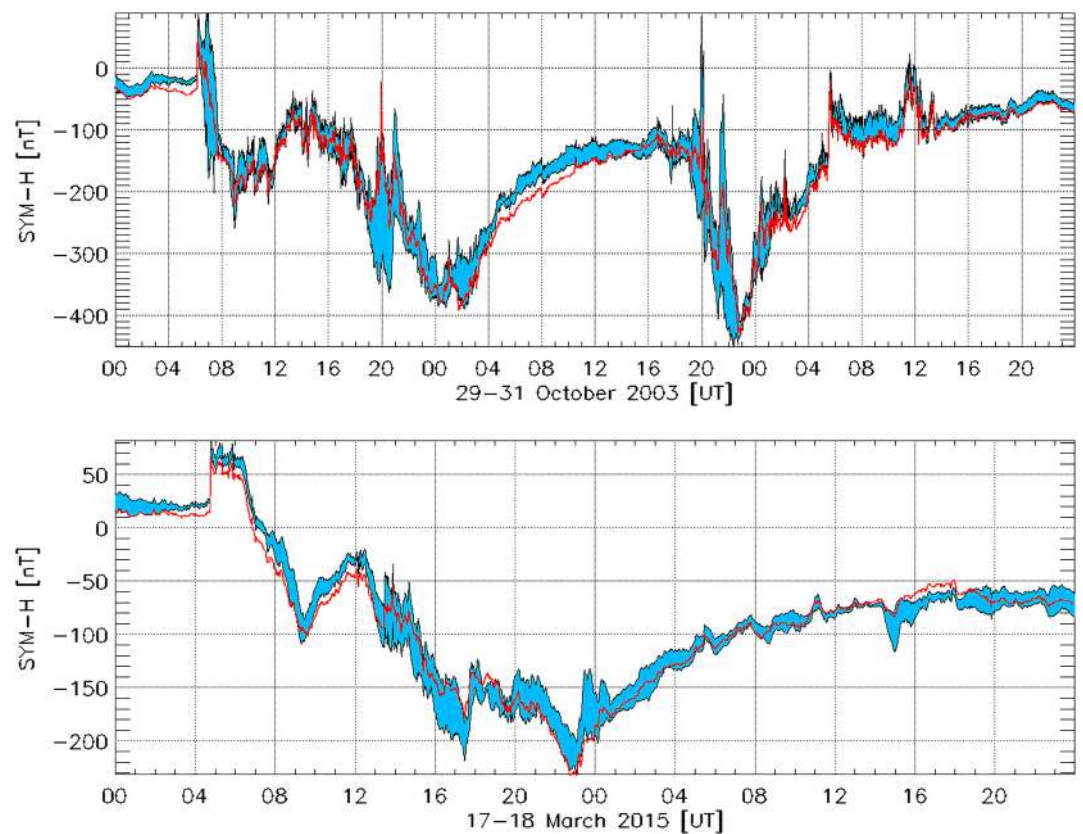


**Figure 9.** Top: SYM-H index for the Halloween event (29–31 October 2003). Bottom: SYM-H index for the St. Patrick event (17–18 March 2015). In blue, the range of possible values for the indices due to the freedom to choose observatories in their definition. The values in blue obtained from Local Disturbance index procedure. In red, the Kyoto WDC published indices.

The LDi index was also evaluated using the SYM-H index to highlight its importance for its good representation of local geomagnetic activity events. The use of 6 out of 10 available magnetic observatories to calculate the SYM-H was scrutinized with the help of LDi data calculated at these observatories.

Figure 6 shows the risk of choosing freely six stations for the SYM-H calculation, one in each of four longitude sectors and HON and MMB that are singles in their sectors (Figure 6). Opposite disturbances at some stations are well observed from 06 to 08 UT on 29 October 2003, which would not yield a good estimation of the magnitude of the event. A further analysis that estimated the SYM-H index from LDi data for both Halloween and Saint Patrick events from 16 different combinations of the observatories of four sectors produced the results shown in Figure 9. It is clear that the range of possible values, in blue, can be considerable, reaching 330 nT (21:37 UT on 30 October 2003) for the Halloween event and 64 nT (13:55 UT on 17 March 2015) for the Saint Patrick event. This is due to the freedom of choice of some observatories in the definition of the procedure to calculate the SYM-H index. Also interesting is the case of the difference between the published SYM-H values and the estimated SYM-H. In this case, the maximum differences are 298 nT (19:57 UT on 29 October 2003) for the Halloween event and 65 nT (23:44 UT on 17 March 2015) for the Saint Patrick event. However, in general, there is a good agreement between the estimated SYM-H index using LDi data and the published SYM-H index for both Halloween and Saint Patrick events.

The local magnetic disturbances that can manifest themselves in the recorded GICs in Spain and South Africa might not be observed at other locations.

**Table 3**

*Classification of Geomagnetic Storms According to Their Severity and the Linear Correlation Coefficient R Between 1-hr Disturbance Values Calculated From Local Disturbance Index and H Component Data For Each Storm at Hermanus Magnetic Observatory. 1-hr Disturbance Value Is the Range Value in 1-hr Interval of 1-Min Data*

Date	MD (nT)	R
29–31 October 2003	Severity > 220	0.997
27–29 October 1991		0.978
15–16 May 2005	130 < MD ≤ 220	0.992
24–25 August 2005		0.989
7–10 November 2004		0.961
21–22 January 2005	80 < MD ≤ 130	0.988
17–18 March 2015		0.963
10–13 September 2005	MD ≤ 80	0.969
17–18 March 2013		0.972

*Note.* Maximum 1-hr disturbance value (MD) in nT, observed in H or LDi data for selected geomagnetic storms, has been used as a proxy for the severity of a geomagnetic storm.

This can be proved by the lack of signature of these local disturbances in some global indices like SYM-H. Then, the LDi index is important for local space weather studies as it indicates the local geomagnetic disturbances without adding contributions from other sources that might have their own different local geomagnetic conditions. The derivation of the LDi index uses a special technique to remove the solar regular variation, similar to the procedure used by observers when hand-scaling geomagnetic indices. This technique does not depend on international quietest days of the month, which are restricted to UT days. It uses the local time at the location of the observatory to classify geomagnetic quiet days by itself. This makes the LDi index totally independent from other sources and suitable for real-time execution to characterize local geomagnetic activity.

## 5. Conclusion

The LDi and its derivative, the LDi, developed in the Northern Hemisphere (Cid et al., 2020), have been validated in the Southern Hemisphere. This validation was based on the availability of GIC data at two South African power stations, Grassridge and Matimba, during Halloween and Saint Patrick's Day geomagnetic storms in 2003 and 2015, respectively. The evaluation of the LDi index was performed using the local horizontal component H recorded at HER and HBK magnetic observatories, and the global SYM-H index.

The results of the derivative of the H component and indices shown in Table 1, Figures 2 and 3 indicate that LDi and LDi indices perform well in the Southern Hemisphere as indicated in Section 4. The forward and central derivatives of the H component are very similar to what is observed with the LDi at HER and HBK. Using 10 selected GIC peaks, five in each of Halloween and Saint Patrick's Day events,  $dH/dt$  or  $d_c H/dt$  and LDi have a very similar performance in now-casting GIC events. The comparative evaluation of the LDi was also conducted using 1-hr magnetic disturbance values calculated from the H component using the LRNS algorithm and the ones calculated from the LDi. Table 3 and Figures 5 and A1 show a good agreement between LRNS and LDi values, and the Pearson correlation coefficient  $R$  is always greater than 0.960 for different groups of magnetic storms that were formed according to the severity of geomagnetic activity.

The comparison of the local LDi index to the global SYM-H index showed the importance of using a local index to characterise local geomagnetic disturbances. Figures 6–9 present the analysis of the freedom of choice of magnetic observatories that contribute data to the SYM-H index derivation, and how this selection can lead to different SYM-H index values. The estimated SYM-H index from LDi data using 16 combinations of stations in four sectors presented in Figure 6 revealed a possible difference of about 300 nT from the published SYM-H index around 20:00 UT on 29 October 2003 during Halloween storm. The validation of the LDi and LDi indices, using magnetic and GIC data from South African magnetic observatories and power stations, has shown that these local indices can be calculated at similar latitudes in the Southern Hemisphere to represent successfully local geomagnetic conditions.

## Appendix A

The following plots of Linear phase Robust Non-linear Smoothing method and Local Disturbance index 1-hr magnetic disturbances at Hermanus magnetic observatory for other selected geomagnetic storms with different degrees of severity support the results in Figure 5.

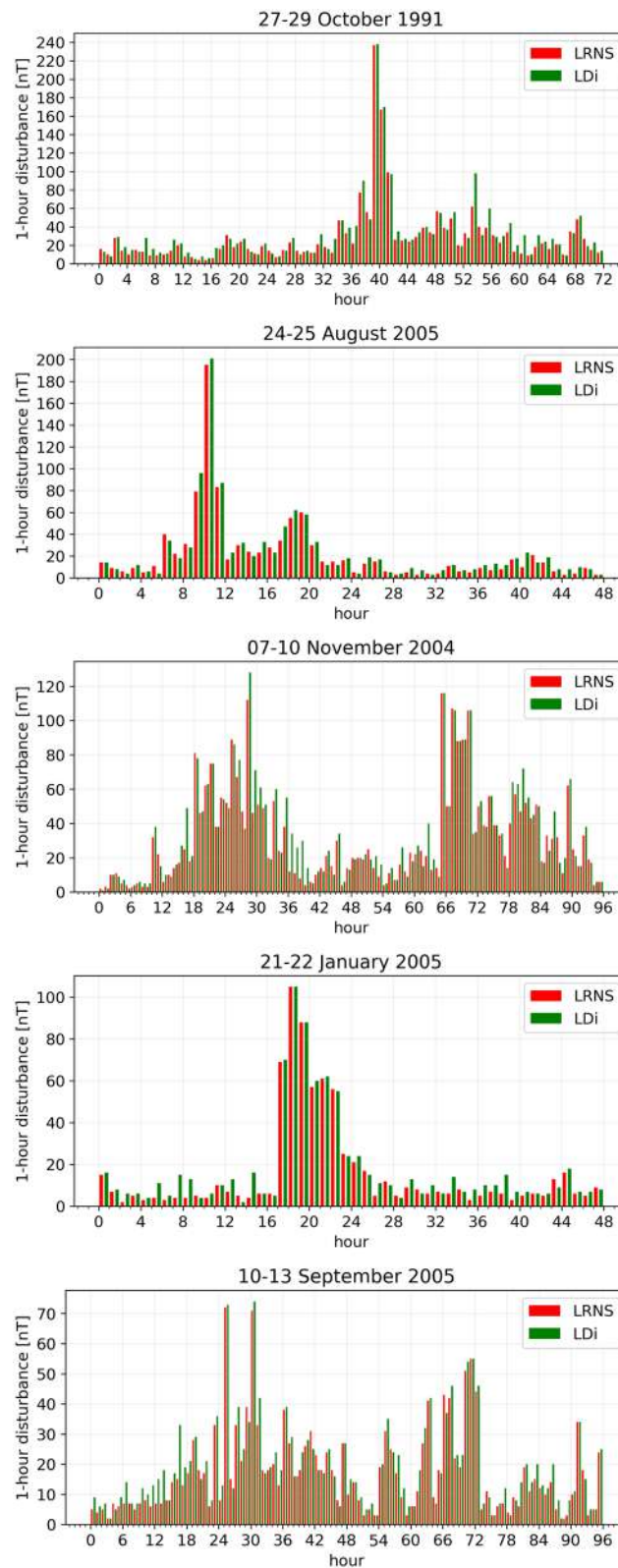


**Figure A1.** Additional plots of Linear phase Robust Non-linear Smoothing method and Local Disturbance index 1-hr magnetic disturbances in the H component at Hermanus magnetic observatory for selected geomagnetic storms with different degrees of severity.

## Data Availability Statement

The software for the LRNS method is available at <http://isgi.unistra.fr/software.php>. The GIC data were provided to us by ESKOM, and interested readers of this paper may access them and other used data via the link: <https://zenodo.org/record/7019253>.

## Acknowledgments

A. Guerrero, C. Cid and E. Saiz acknowledge the support by the project PID2020-119407GB-I00/AEI/10.13039/501100011033. We also acknowledge the following data sources: (a) the SYM-H data obtained through the Kyoto WDC (<http://wdc.kugi.kyoto-u.ac.jp/>), (b) the magnetic data from ground magnetometers freely accessible from the INTERMAGNET database (<http://www.intermagnet.org/>), (c) the GIC data recorded by the ESKOM Solar Storm Resilience Team at Grassridge and Matimba power stations and special thanks to the teams of the magnetic observatories who recorded the data used in this work. We would like to thank Reviewers for taking the time and effort necessary to review the manuscript. We sincerely appreciate all valuable comments and suggestions, which helped us to improve the quality of the manuscript.

## References

- Bartels, J., & Veldkamp, J. (1949). International data on magnetic disturbances, first quarter, 1949. *Journal of Geophysical Research*, *54*(3), 295–299. <https://doi.org/10.1029/JZ059i003p00423>
- Boteler, D. H., & Pirjola, R. J. (2017). Modeling geomagnetically induced currents. *Space Weather*, *15*(1), 258–276. <https://doi.org/10.1002/2016SW001499>
- Cid, C., Guerrero, A., Saiz, E., Halford, A. J., & Kellerman, A. C. (2020). Developing the LDi and LCi geomagnetic indices, an example of application of the AULS framework. *Space Weather*, *18*(1), e2019SW002171. <https://doi.org/10.1029/2019SW002171>
- Clilverd, M. A., Rodger, C. J., Brundell, J. B., Dalzell, M., Martin, I., Mac Manus, D. H., & Thomson, N. R. (2020). Geomagnetically induced currents and harmonic distortion: High time resolution case studies. *Space Weather*, *18*(10), e2020SW002594. <https://doi.org/10.1029/2020SW002594>
- Cnossen, I., & Matzka, J. (2016). Changes in solar quiet magnetic variations since the Maunder Minimum: A comparison of historical observations and model simulations. *Journal of Geophysical Research: Space Physics*, *121*(10), 10520–10535. <https://doi.org/10.1002/2016JA023211>
- Davis, T. N., & Sugiura, M. (1966). Auroral electrojet activity index AE and its universal time variations. *Journal of Geophysical Research*, *71*(3), 785–801. <https://doi.org/10.1029/JZ071i003p00785>
- Falayi, E. O., Ogunmodimub, A. O., Bolajic, O. S., Ayandaa, J. D., & Ojoniyi, O. S. (2017). Investigation of geomagnetic induced current at high latitude during the storm-time variation. *NRIAG Journal of Astronomy and Geophysics*, *6*(1), 131–140. <https://doi.org/10.1016/j.nrjag.2017.04.010>
- Freedman, D., Pisani, R., & Purves, R. (2007). *Statistics (international student edition)* (4th ed.). WW Norton & Company.
- Gaunt, C. T., & Coetzee, G. J. (2007). Transformer failures in regions incorrectly considered to have low GIC-risk. *2007 IEEE Lausanne Power Tech*, (pp. 807–812). IEEE.
- Gilbert, J. L. (2005). Modeling the effect of the ocean-land interface on induced electric fields during geomagnetic storms. *Space Weather*, *3*, S04A03. <https://doi.org/10.1029/2004SW000120>
- Häkkinen, L. V., Pulkkinen, T. I., Pirjola, R. J., Nevanlinna, H., Tanskanen, E. I., & Turner, N. E. (2003). Seasonal and diurnal variation of geomagnetic activity: Revised Dst versus external drivers. *Journal of Geophysical Research*, *108*(A2), 1060. <https://doi.org/10.1029/2002JA009428>
- Halford, A. J., Kellerman, A. C., Garcia-Sage, K., Klenzing, J., Carter, B. A., Brett, A., et al. (2019). Application usability levels: A framework for tracking project product progress. *Journal of Space Weather and Space Climate*, *9*(11), A34. <https://doi.org/10.1051/swsc/2019030>
- Hattingh, M., Loubser, L., & Nagtegaal, D. (1989). Computer K-index estimation by a new linear-phase, robust, non-linear smoothing method. *Geophysical Journal International*, *99*(3), 533–547. <https://doi.org/10.1111/j.1365-246X.1989.tb02038.x>
- Iyemori, T. (1990). Storm-time magnetospheric currents inferred from mid-latitude geomagnetic field variations. *Journal of Geomagnetism and Geoelectricity*, *42*(11), 1249–1265. <https://doi.org/10.5636/jgg.42.1249>
- Iyemori, T., & Rao, D. (1996). Decay of the Dst field of geomagnetic disturbance after substorm onset and its implication to storm-substorm relation. *Annales Geophysicae*, *14*(6), 608–618. <https://doi.org/10.1007/s00585-996-0608-3>
- Karinen, A., & Mursula, K. (2005). A new reconstruction of the Dst index for 1932–2002. *Annales Geophysicae*, *23*(2), 475–485. <https://doi.org/10.5194/angeo-23-475-2005>
- Kozyreva, O. V., Pilipenko, V. A., Belakhovsky, V., & Sakharov, Y. A. (2018). Ground geomagnetic field and GIC response to March 17, 2015, storm. *Earth, Planets and Space*, *70*(157), 1–13. <https://doi.org/10.1186/s40623-018-0933-2>
- Mursula, K., Holappa, L., & Karinen, A. (2008). Correct normalization of the Dst index. *Astrophysics and Space Sciences Transactions*, *4*(2), 41–45. <https://doi.org/10.5194/astra-4-41-2008>
- Schrijver, C. J., & Mitchell, S. D. (2013). Disturbances in the US electric grid associated with geomagnetic activity. *Journal of Space Weather and Space Climate*, *3*, A19. <https://doi.org/10.1051/swsc/2013041>
- Sugiura, M. (1964). *Hourly values of equatorial Dst for the IGY*. Annals of the International Geophysical Year. (Vol. 35).
- Thomson, A. W. P., Gaunt, C. T., Cilliers, P., Wild, J. A., Opperman, B., McKinnell, L.-A., et al. (2010). Present day challenges in understanding the geomagnetic hazard to national power grids. *Advances in Space Research*, *45*(9), 1182–1190. <https://doi.org/10.1016/j.asr.2009.11.023>
- Viljanen, A., Nevanlinna, H., Pajunpää, K., & Pulkkinen, A. (2001). Time derivative of the horizontal geomagnetic field as an activity indicator. *Annales Geophysicae*, *19*(9), 1107–1118. <https://doi.org/10.5194/angeo-19-1107-2001>
- Viljanen, A., Wintoft, P., & Wik, M. (2015). Regional estimation of geomagnetically induced currents based on the local magnetic or electric field. *Journal of Space Weather and Space Climate*, *5*, A24. <https://doi.org/10.1051/swsc/2015022>
- Wanliss, J. A., & Showalter, K. M. (2006). High-resolution global storm index: Dst versus SYM-H. *Journal of Geophysical Research*, *111*(2), 1–10. <https://doi.org/10.1029/2005JA011034>